

# 6R cuspidal robots: kinematic issues and guidelines for path planning and design

Journal Title  
XX(X):1–18  
©The Author(s) 2023  
Reprints and permission:  
[sagepub.co.uk/journalsPermissions.nav](http://sagepub.co.uk/journalsPermissions.nav)  
DOI: 10.1177/ToBeAssigned  
[www.sagepub.com/](http://www.sagepub.com/)



Durgesh Haribhau Salunkhe<sup>1</sup> and Tobias Marauli<sup>2</sup> and Andreas Müller<sup>2</sup> and Damien Chablat<sup>1</sup> and Philippe Wenger<sup>1</sup>

## Abstract

Cuspidal serial robots can change inverse kinematic solutions (IKS) without crossing singularities in the joint space because they have multiple IKS in a singularity-free region. This property of robots has been researched for over three decades but has not been taken seriously in consideration while designing new robots. The presented work points out issues related to nonsingular change of IKS and path planning specific to the cuspidal robots that are present in existing commercial robots used in various applications. The multiple IKS at the initial end-effector pose allows the user to choose an initial IKS that may lead to a continuous and repeatable path. We analyze in detail how the choice of the initial IKS affects the feasibility and repeatability of the prescribed path. Cuspidal robots can be used safely if the workspace is analyzed taking into account the cuspidality property. For these reasons, we propose a methodology for path testing and planning that considers different path scenarios. Given the rise of unconventional designs in 6R robots, the identification of cuspidal properties in the design phase of a robot is of paramount importance. We recall all the known criteria for cuspidality and propose new methods to decide if a given 6R robot is cuspidal. Accordingly, a practical guideline is proposed for deciding the cuspidality of a generic 6R robot.

## Keywords

Cuspidal robots, Nonsingular change of solutions, kinematics, serial robots, path planning

## 1 Introduction

In recent years, the robotics industry has shown an inclination toward exploring unconventional designs for 6R robots. The widely implemented design with a wrist partitioned geometry, also known as the 'Puma-type' or 'anthropomorphic robot', is expensive to assemble and sensitive to manufacturing errors. This is attributed to the reason that the last three axes intersect at a point forming a wrist architecture. Almost all collaborative robots across the industry have adopted the introduction of an offset in the wrist such as FANUC CRX-10ia/L, Yaskawa HC10DTP, and Universal Robots to name a few. The wrist partitioned assembly is a nongeneric geometry of a 6R robot that results in the well-known kinematic properties such as simplified inverse kinematic model Pieper (1968) and every IKS separated by singularities in the joint space Wenger and Chablat (2022). These special kinematic properties are not guaranteed if one deviates from this architecture. An offset in the wrist may lead to an overlooked property called cuspidality, which is highlighted in this paper. Cuspidal robots refer to robots whose joint space has at least one singularity-free connected region, referred to as *aspect* Borrel and Liegeois (1986); Wenger (1992), with multiple inverse kinematic solutions (IKS). This enables the robot to travel between two IKS without crossing inverse kinematic singularities, and this property is termed cuspidality. Historically, the term *cuspidal* comes from the fact that a projection of the critical values (the forward kinematics map of the singularities) has cusps, which is a

necessary and sufficient condition for 3R orthogonal robots to be cuspidal El Omri and Wenger (1995). This condition was later extended to generic 3R robots Salunkhe et al. (2022b). This term was used in the context of 6R robots by Wenger and Chablat (2022) and Wenger (1997).

The advantage of anthropomorphic robots is that their IKS can be calculated in closed form and thus the computation is fast and accurate. A closed-form solution for similar architectures, but with an offset in the wrist is presented in Gosselin and Liu (2014); Trinh et al. (2015); Zohour et al. (2021). These works confirm that robots with offset in the wrist have more than 8 IKS. It is shown for these robots that there exist multiple regions with different numbers of IKS in the workspace separated by critical values Salunkhe et al. (2023). Such a workspace presents the possibility of moving from one region to another, i.e. crossing critical values, which makes the path planning problem harder to handle.

Issues in path planning for cuspidal robots were first recognized by Wenger (2004) in 3R robots. This work highlighted the importance of considering different scenarios, specific to path planning of cuspidal robots. Recently, a few issues in path planning of Jaco Gen2 (version with a non-spherical wrist) were presented by Verheyen (2021) where the robot jumped off the desired trajectory. The kinematic analysis presented in Salunkhe et al. (2023) confirmed that this robot is cuspidal. The work also illustrated the relation between the issues in path planning and the cuspidal property of the robot. There has been a dearth of attention towards cuspidality while

<sup>1</sup>Nantes Université, École Centrale Nantes, CNRS, LS2N, UMR 6004, 44000 Nantes, France

<sup>2</sup>Institute of Robotics, Johannes Kepler University Linz, Austria  
Prepared using sagej.cls [Version: 2017/01/17 v1.20]

## Corresponding author:

Philippe Wenger, S404 S Building, Ecole Centrale de Nantes, 1, Rue de

designing a 6R robot, which has led to an increasing number of cuspidal robots in the market. As the deployment of cuspidal robots becomes ubiquitous, it is imperative to have a practical guideline for path planning that takes cuspidality into account.

Deciding upon the cuspidal nature of 6R robots is a challenging task as the singularities exist in four-dimensional joint space. Few industrial robots were analyzed individually for studying the cuspidal nature [Wenger and Chablat \(2022\)](#); [Capco et al. \(2020\)](#) but no work was published regarding a generic 6R robot until recently. The latest work on deciding cuspidality was presented in [Chablat et al. \(2022\)](#). The presented algorithm is generic and certified, but very hard to implement.

The main contributions presented in the article are:

1. Issues in path planning of commercial cuspidal robots (Section 4): the issues in unique identification of IKS in commercial software, and consequences of cuspidality on path planning are presented. Several types of paths and scenarios occurring in cuspidal robots are demonstrated to highlight the importance of avoiding cuspidal robots in collaborative tasks.
2. Path planning algorithm (Section 4.4): we propose a practical path planning algorithm taking non-cuspidal as well as cuspidal robots into account. It considers several scenarios specific to the path planning of cuspidal robots.
3. Deciding algorithm (Section 5): a practical algorithm to decide if given D-H parameters correspond to a cuspidal robot or not is proposed. It combines the previously known results along with analysis of the determinant of the Jacobian matrix to accelerate the decision time.

This paper is organized as follows: Section 2 presents the chronology and relevant work in the field of kinematic analysis of 6R robots. Section 3 puts forth the necessary terminologies as well as the background for the work presented in the sections to follow. Section 4 discusses the issues in path planning of cuspidal robots. The path-planning algorithm of cuspidal robots is discussed here in detail. A few examples from existing commercial cuspidal robots are shown to highlight the importance of the algorithm. In section 5, the practical algorithm for deciding cuspidality is presented. Later, we present the classification of existing robots based on cuspidality. We conclude the presented work with a few remarks on cuspidal robots and their consequences on path planning.

## 2 Related work

This section summarizes the related work on the topics of inverse kinematics, cuspidal robots, and path planning methodologies of 6R robots.

### 2.1 Kinematic analysis

The work of [Pieper \(1968\)](#) presented the inverse kinematic model (IKM) of a 3R robot as an intersection of a conic with a unit circle. This analysis was used in extending the

cuspidality analysis for 3R robots [Salunkhe et al. \(2022b\)](#); [Thomas \(2015\)](#); [Salunkhe et al. \(2022a\)](#); [Smith and Lipkin \(1990\)](#). In 1986, [Primrose \(1986\)](#) proved that 6R robots have up to 16 solutions over  $\mathbb{C}$  using projective geometry. One of the most recent advances in the inverse kinematics of 6R robots was presented by [Husty et al. \(2007\)](#) where the geometric interpretation of the IKM was presented. The advantage of this method is that it uses equations linear in all but two variables, and thus is fast and accurate. This method was extended for robots with prismatic joints by [Capco and Manongsong \(2019\)](#).

### 2.2 Cuspidal robots

Before 1988, it was believed that the IKS of a 6R robot were always separated by the locus of critical points of the forward kinematic map [Borrel and Liegeois \(1986\)](#). This idea was discarded in 1988 and two counter-examples were presented in [Innocenti and Parenti-Castelli \(1998\)](#) establishing the existence of cuspidal robots. Cuspidality was then also shown in 3R robots by [Burdick \(1989\)](#). As the wrist partitioned geometries of 6R robots are noncuspidal and the IKS of these robots are thus well separated by singularities, the implications of 6R cuspidal robots were not studied rigorously. The 3R robots, on the other hand, have extensive results based on cuspidality [Wenger \(1992\)](#); [El Omri and Wenger \(1995\)](#). Figure 1 illustrates an example of nonsingular change of solutions. Figure 1a shows the singularities in the joint space parameterized by  $\theta_2 - \theta_3$  only as  $\theta_1$  does not affect the singularities. In Figure 1b, the critical values in  $\rho = \sqrt{x^2 + y^2}$  and  $z$  are shown. The workspace is parameterized in  $\rho$  and  $z$  as they are functions of  $\theta_2$  and  $\theta_3$  only. The term *cuspidal* robots was coined since a nonsingular change of solutions in the joint space is equivalent to encircling a cusp point of the locus of critical values of the forward kinematic map projected onto a surface in the workspace of the robot. It was proved for orthogonal 3R robots, i.e. an arrangement with three mutually perpendicular revolute axes, that the existence of a cusp point was a necessary and sufficient condition to be cuspidal [El Omri and Wenger \(1995\)](#). The complete parameter space was mapped leading to the validation of the proof of this condition. [Wenger \(1998\)](#) and [Baili et al. \(2004\)](#) used homotopy classification to further analyze 3R robots. [Baili et al. \(2004\)](#) presented the classification of orthogonal robots in terms of the number of cusps while [Paganelli \(2008\)](#) studied the classification of 3R robots concerning the aspects thus extending the previous work [Wenger \(1998\)](#).

The IRB 6400C robot from ABB was first introduced in the assembly lines to save the space required by robots by changing the first axis positioning. This robot was then pulled back from the assembly lines and the reasons were not clear. It was later reported that this robot was indeed cuspidal [Wenger and Chablat \(2022\)](#), and the authors suspect that the issues related to path planning in cuspidal robots were encountered by the engineers. Another robot, GMF150, was analyzed by [Wenger \(1997\)](#), and it is concluded that this robot is cuspidal in theory, but due to strong joint limits, the robot operates in a 2 IKS region such that the IKS are always separated by a singularity. A major change from the conventionally deployed design came with the introduction of an offset in the wrist of anthropomorphic

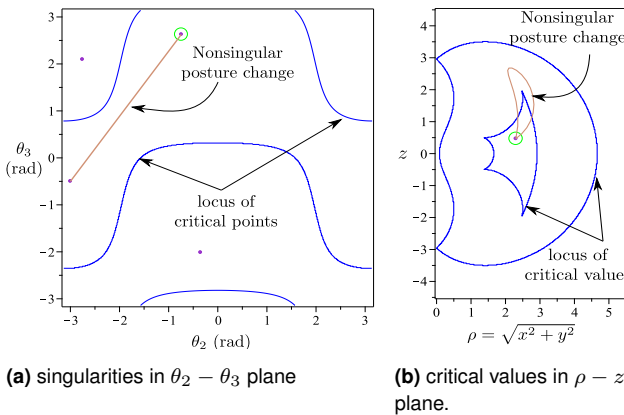


**Figure 1.** An example of nonsingular change of solution in joint space and workspace.

Robot parameters:

$$\mathbf{d} = [0, 1, 0], \mathbf{a} = [1, 2, 3/2], \alpha = [-\frac{\pi}{2}, \frac{\pi}{2}, 0].$$

Path in the joint space ( $\theta_2, \theta_3$ ): from  $(-0.742, 2.628)$  to  $(-3, -0.5)$ .

robots, and the introduction of three parallel axes in the 6R robot. These designs are so popular that almost all robot manufacturing companies have a version of this such as the FANUC CRX series, UR5 from Universal Robots, Yaskawa's HC10DTP, and Gen Lite3 from Kinova Robotics. It is reported that robots similar to the UR5 architecture are non-cuspidal and the determinant of the Jacobian matrix of such robots factor resulting in partitions in the joint space Capco et al. (2020). This results from the fact that UR5-like robots have a 3R planar subchain. Since anthropomorphic robots vary from this structure, adding an offset in the wrist almost always leads to a cuspidal design, as shown in Section 5. An example of such a design that deviates from the wrist-partitioned anthropomorphic architecture is JACO Gen2 (version with non-spherical wrist) which is reported to be cuspidal Salunkhe et al. (2023).

Deciding on cuspidality for a given robot allows a designer to make better decisions based on the advantages of the designs and challenges in the path planning of cuspidal robots. The identification of cuspidality in 3R robots has been completely presented in El Omri and Wenger (1995) and Salunkhe et al. (2022b) from which the necessary and sufficient condition for a 3R robot to be cuspidal was put forth. This work also presented proof for the existence of reduced aspects (see section 3) in generic 3R robots. No results on the reduced aspects are available for 6R robots. The cuspidality analysis of 3R robots can be extended to 6R robots with a wrist at the end or the beginning as the rotation and translation part of the end effector pose (EE-pose) is decoupled for these simplified architectures. There has been no attempt to develop a unified framework to decide cuspidity for generic 6R robots before 2022, but few industrial robots were individually analyzed for cuspidal behavior.

Recently, a certified algorithm was presented for deciding cuspidity for nonredundant nR robots Chablat et al. (2022). It implements various algorithms in computer algebra and is computationally expensive at its current stage. Though certified, this algorithm has no implementation for 6R robots at present, and cannot be used with collision constraints.

### 3 Preliminaries

In this section, we discuss the definitions relevant to cuspidal robots as well as path planning in cuspidal robots.

#### 3.1 Inverse kinematics

The subspace of  $SE(3)$  formed by the reachable poses of a given 6R robot is called the workspace of the robot,  $\mathcal{W} \subset SE(3)$ . The joint configuration of a robot is denoted as  $\mathbf{q}$  and is a point in the joint space,  $\mathcal{J} \subseteq \mathbb{T}^6$ , where,  $\mathbb{T}^n$  is an n-torus. Let  $\mathbf{x}$  be the EE-pose in  $SE(3)$  corresponding to  $\mathbf{q}$ . The mapping between  $\mathcal{J}$  and  $\mathcal{W}$ , denoted by  $f : \mathcal{J} \rightarrow \mathcal{W}$ , defines the forward kinematics

$$\mathbf{x} = f(\mathbf{q}), \mathbf{x} \in \mathcal{W}, \mathbf{q} \in \mathcal{J}.$$

The elements in the pre-image  $f^{-1}(\mathbf{x})$  are the inverse kinematic solutions (IKS) of  $\mathbf{x}$ . In this paper, original D-H parameters are used Denavit and Hartenberg (1955). The conventions used in this parameterization are presented in Figure 2.

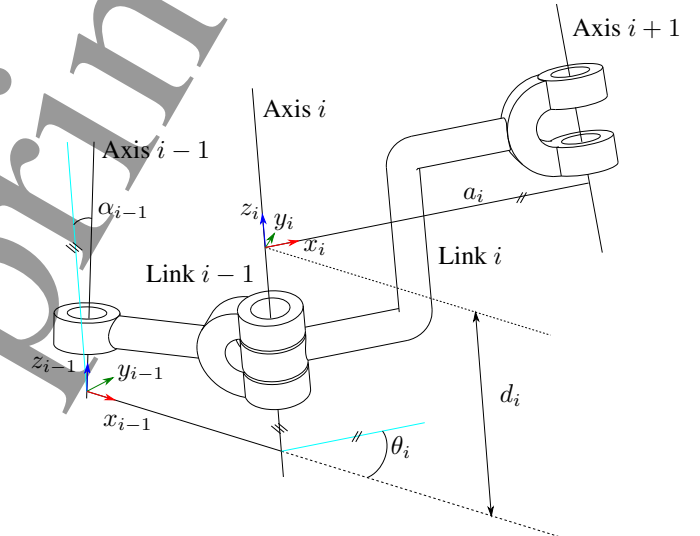


**Figure 2.** Conventions of the original D-H parameters used in this work.

The algorithms discussed in Section 5 implement HuPf algorithm to obtain the IKS of a generic 6R robot. Readers are encouraged to refer to Capco and Manongsong (2019); Husty et al. (2007) for detailed implementation where the IKM is presented as an algorithm. A comparison of the HuPf algorithm to other algorithms for inverse kinematics was performed in Angerer and Hofbaur (2013) for industrial setup. As accuracy is more important than speed for deciding cuspidity, the HuPf algorithm is the most reliable algorithm for cuspidity analysis of 6R robots.

#### 3.2 Singularities in serial robots

The set of singularities ( $\mathcal{S}$ ) contain all critical points of  $f$  in  $\mathcal{J}$  that correspond to the configurations in the joint space where the Jacobian of the forward kinematic map,  $\mathbf{J}$ , loses rank, i.e. when the determinant of  $\mathbf{J}$  is zero ( $\det(\mathbf{J}) = 0$ ). The critical values are the images of the critical points in  $\mathcal{W}$ . Kohli and Spanos (1985) showed that the roots of the univariate polynomial used to solve the inverse kinematics

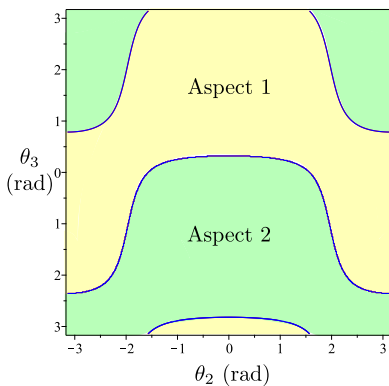


**Figure 3.** The two singularity-free connected regions, called aspects, in joint space for a 3R robot

Robot parameters:  $d = [0, 1, 0]$ ,  $a = [1, 2, \frac{3}{2}]$ ,  $\alpha = [-\frac{\pi}{2}, \frac{\pi}{2}, 0]$

have a multiplicity of 2 or more for a 3R robot. This result can be extended to 6R robots too as there is always a loss/gain of IKS upon crossing the locus of critical values.

It is known that the singularities of 6R robots are independent of the first joint angle,  $\theta_1$ , and the last joint angle,  $\theta_6$ , Innocenti and Parenti-Castelli (1998). This allows us to reduce the 6-dimensional joint space to  $\mathbb{T}^4$  parameterized by  $\theta_2, \theta_3, \theta_4$  and  $\theta_5$ . In the following part of the article,  $\mathcal{J} \subseteq \mathbb{T}^4$  will denote the joint space parameterized by  $\theta_i, i \in \{2, 3, 4, 5\}$ .

**Aspect:** The aspects are the largest singularity-free connected regions in the joint space of a robot Borrel and Liegeois (1986). Figure 3 shows two aspects in the joint space of a 3R robot. The joint space is parameterized in  $\theta_2$  and  $\theta_3$  only as the singularities of 3R robot are independent of  $\theta_1$  Burdick (1989).

**Generic robots:** Robots whose locus of critical points form a smooth manifold are termed generic robots Pai and Leu (1992). Self-intersection of the singularity manifold qualifies it to be a nongeneric robot.

**Cusp:** A cusp is a point in the locus of critical values of a 3R robot that satisfies the following conditions El Omri and Wenger (1995):

$$\begin{aligned} M(t_3, R, z) &= 0 \\ \frac{\partial M}{\partial t_3}(t_3, R, z) &= 0 \\ \frac{\partial^2 M}{\partial t^2}(t_3, R, z) &= 0 \end{aligned} \quad (1)$$

where, for an end-effector (EE) position  $(x, y, z)$ ,  $R = x^2 + y^2 + z^2$ , and  $t_3 = \tan \frac{\theta_3}{2}$ . The function,  $M(t_3, R, z)$ , is a polynomial of degree four in  $t_3$ . This polynomial is obtained by eliminating the joint variable  $t_2$  from the forward kinematic function. Moreover, the cusp also has to satisfy:

$$\frac{\partial^3 M}{\partial t_3^3}(t_3, R, z) \neq 0 \quad (2)$$

to exclude quadruple roots. However, it was shown in Pai and Leu (1992) that quadruple roots cannot exist in generic 3R robots, and the above condition is thus always satisfied here. So, in the context of a generic 3R robot, the cusp in the

workspace relates only to satisfying (1).

**IKS set:** Denote with

$$\mathcal{I}_x = \{\mathbf{q} \in \mathbb{T}^n \mid \mathbf{x} = \mathbf{f}(\mathbf{q})\} \quad (3)$$

the set of IKS for a given end effector pose  $x$  of a  $n$ -DOF robot. The IKS can be computed using e.g. the HuPf-algorithm Husty et al. (2007) or a robot-specific approach such as Gosselin and Liu (2014) for the Kinova Jaco robot. For a non-redundant robot, i.e.  $\dim \mathcal{W} = \dim \text{Im}(f) \leq n$ , the IKS set consists of a finite number  $n_x$  of IKS i.e.  $\mathcal{I}_x = \{\mathbf{q}_1, \dots, \mathbf{q}_{n_x}\}$ .

**Set of candidate solutions:** A necessary condition for two distinct IKS to belong to the same aspect, is that the determinant of the Jacobian has the same sign. We obtain a reduced set from the set of all IKS at a given pose, which qualifies after the necessary condition is imposed. This reduced set of IKS is defined as the set of candidate IKS for an initial solution  $\mathbf{q}_0$  and EE-pose  $x$  and is introduced as:

$$\mathcal{R}_{\mathbf{q}_0, x} := \{\mathbf{q} \in \mathcal{I}_x \mid \text{sign}(\det \mathbf{J}(\mathbf{q}_0)) = \text{sign}(\det \mathbf{J}(\mathbf{q}))\} \quad (4)$$

**Nonsingular change of solutions:** Let  $\mathbf{q}_1$  and  $\mathbf{q}_2$  be two IKS for the EE-pose  $x$  and  $\sigma(\mathbf{q}_1, \mathbf{q}_2, t)$  be a path between these two points, where  $t \in [0, 1]$  is a parameter such that  $\sigma(\mathbf{q}_1, \mathbf{q}_2, 0) = \mathbf{q}_1$  and  $\sigma(\mathbf{q}_1, \mathbf{q}_2, 1) = \mathbf{q}_2$ .  $\sigma(\mathbf{q}_1, \mathbf{q}_2, t)$  is defined as a nonsingular change of solutions if and only if:

$$\sigma(\mathbf{q}_1, \mathbf{q}_2, t) \cap S = \emptyset \mid \mathbf{q}_1, \mathbf{q}_2 \in \mathcal{R}_{\mathbf{q}_0, x}, \forall t \quad (5)$$

**Connectivity problem:** The problem of finding a path connecting two IKS  $\mathbf{q}_i, \mathbf{q}_j \in \mathcal{R}_{\mathbf{q}_0, x}$ ,  $i \neq j$ , in the same aspect while satisfying (5) is referred to as the connectivity problem. Two IKS solving the connectivity problem are called 'connected'.

**Cuspidal robots:** Cuspidal robots without collision or joint limit constraints can be defined as robots that have at least one aspect with more than one IKS. Alternatively, it can be defined as a robot for which there exists a nonsingular change of solutions.

$$\exists \sigma(\mathbf{q}_1, \mathbf{q}_2, t) \cap S = \emptyset \mid \mathbf{q}_1, \mathbf{q}_2 \in \mathcal{R}_{\mathbf{q}_0, x} \quad (6)$$

**Repeatable path:** A closed path in the workspace is *repeatable* if the path can be executed infinitely many times. A repeatable path can involve a nonsingular change of solutions.

**Regular closed path:** A regular closed path is a repeatable path such that the initial IKS is the same as the final IKS. Such a path is a closed loop in the workspace as well as in the joint space.

**Non-repeatable path:** A closed path in the workspace is *non-repeatable* path if the path can be executed only once. The initial IKS of such a path cannot be the same as the final IKS (as it would be a regular closed path). Thus, a non-repeatable path is necessarily a nonsingular change of solutions and thus a property of cuspidal robots.

*Infeasible (resp. feasible) path:* A path defined in the workspace that cannot (resp. can) be traversed starting from a given IKS without discontinuity is referred to as an infeasible (resp. feasible) path.

## 4 Path planning for cuspidal robots

In this section, we present the different issues occurring due to the presence of multiple regions with different numbers of IKS in the workspace of a cuspidal robot. Different scenarios are put forth to highlight the classification of different types of paths specific to cuspidal robots. A path-planning algorithm for cuspidal robots is then presented at the end of the section. The proposed algorithm can be implemented on existing commercial cuspidal robots to mitigate the issues in path planning.

### 4.1 Issues with IKS identification

The wrist partitioned 6R robot such as KUKA KR5 has eight IKS and the  $\det(\mathbf{J})$  of such robots factors into three components (detailed in section 5.2.2). These IKS can be unambiguously identified according to the sign of each factor of  $\det(\mathbf{J})$ . If we denote the elbow position, shoulder position, and wrist position with boolean value, then the eight configurations (three factors with boolean values,  $2^3 = 8$ ) for such a robot are shown in Figure 4. Changing from one configuration to another necessarily means that the two IKS are separated by a singularity such that the ‘operation mode’ does not change unless we cross the singularity. A configuration allows one to identify the operation mode of the robot without ambiguity. This can act as a type of classification when the configurations are identified by geometric differences, e.g. elbow up, shoulder right, etc. An IKS on the other side is simply a pre-image of the pose in the workspace. It is to be noted that a geometric interpretation may not be always possible for configurations. For example, in a 3R noncuspidal robot with four real IKS, the solutions are separated by singularities, but these IKS do not necessarily hold an observable distinction. In such case a given configuration can be checked for the aspect in which it belongs, and it can be assured that the robot will stay in this configuration unless we have crossed a singularity. An example of such a robot is shown in Figure 5a, where the four IKS are separated by the singularities allowing one to claim that there are four configurations of the robots. Figure 5b on the other side is an example of a cuspidal robot with four IKS separated into 3 aspects. The two IKS in the same aspect in this figure cannot be uniquely identified, and thus cannot be classified as a configuration.

Numerical methods to calculate the IKS of a generic robot are widely used including in open path planning libraries. When planning a path for a cuspidal robot, a sudden jump off the path can occur if an IKS is missed along the path. This can prove to be catastrophic and thus analytic solutions or algebraic methods need to be used to get all the IKS. We study the case of IKS identification attempted by FANUC on their CRX-10ia/L robot. This robot comes with commercial software ROBOGUIDE® from FANUC for analyzing different IKS and simulating the robot. We know that the CRX-10ia/L robot has up to sixteen IKS, but the

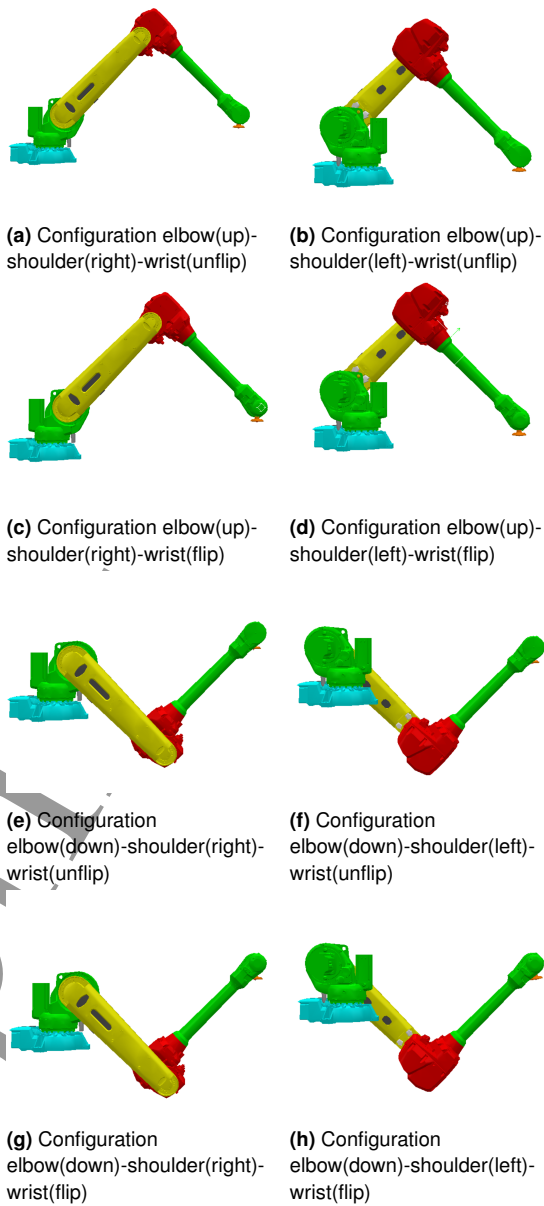
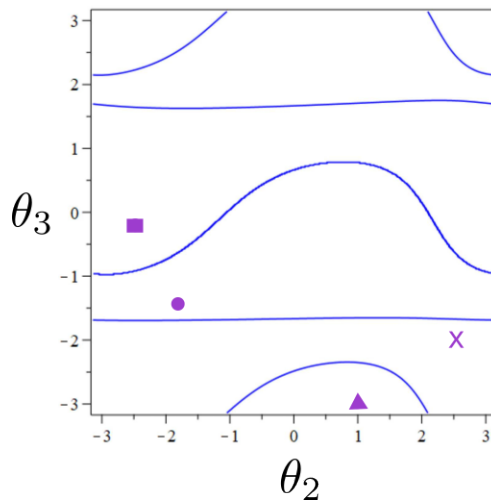


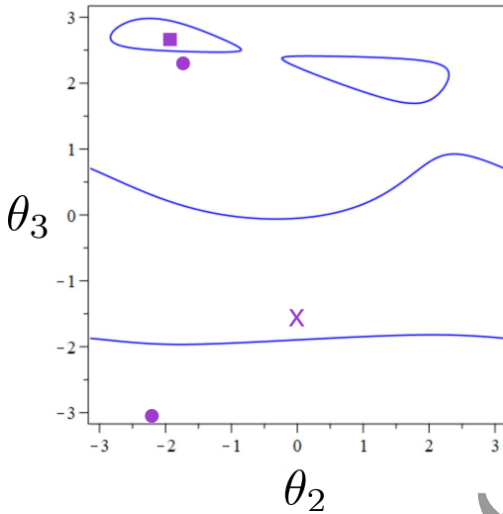
**Figure 4.** The eight configurations of a wrist-partitioned anthropomorphic robot.

software presents up to eight solutions at any given EE-pose, and how the other eight IKS are discarded is unclear. Apart from missing IKS, the software unconventionally assigns a configuration to the eight solutions. Conventionally, the eight configurations are identified as (N/Y)(R/L)(U/D) meaning (No/Yes (flip) - Right/Left (shoulder) - Up/Down (elbow)) as presented in Figure 4. Contrary, ROBOGUIDE® software classifies the configurations in (N/F)(U/D)(T/B) (No flip/Flip - Up/Down (elbow) - Top/Bottom (shoulder)), and this classification is ambiguous. We investigate the issues with unique identification of IKS by considering an example of EE-pose in ROBOGUIDE®, with the Cartesian coordinates as:

X = -467.719 mm, Y = 313.112 mm, Z = -173.618 mm, W = -179.398 degree, P = -0.804 degree, R = -3.321 degree  
Upon experimentation with the software, it is confirmed that the configuration as classified by the software does not necessarily change while traversing a path between two IKS.



(a) Joint space of a noncuspidal robot with 4 IKS in 4 aspects. The IKS in the same aspect have the same symbols.



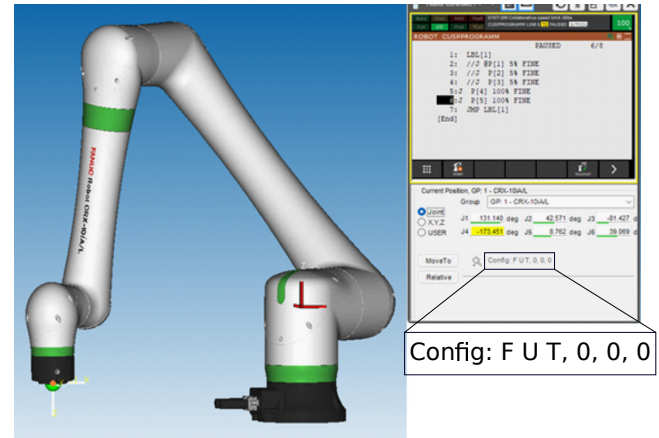
(b) Joint space of a cuspidal robot with 4 IKS existing in 3 aspects. The IKS in the same aspect have the same symbols.

**Figure 5.** Joint space of two robots highlighting cases where a unique identification of IKS is possible or not possible.

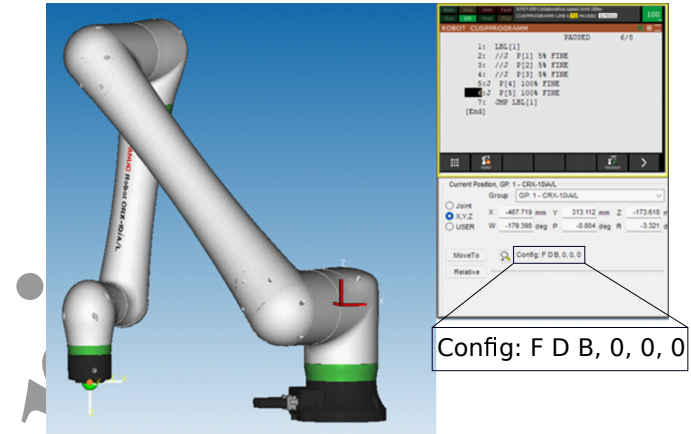
The ambiguity in the configuration classification is shown by two of the IKS as displayed by ROBOGUIDE® in Figure 6. Figure 6a is classified as FUT configuration which is interpreted as Flip (yes), Up (elbow), and Top (shoulder) while the Figure 6b is classified as FDB which can be interpreted as Flip-Down-Bottom configuration. It can be seen that the posture for Figure 6b does not correspond to the elbow-down configuration. This is a misinterpretation of the configuration and can create confusion during the path planning of such robots. The issue for cuspidal robots is not the mislabeling of the configuration, but the absence of the possibility of unique identification of IKS in cuspidal robots.

## 4.2 Types of paths

Different algorithms that can be used for path planning of noncuspidal robots have been presented in Gutierrez et al. (2022). In a wrist-partitioned 6R robot, a given path can be declared infeasible due to multiple reasons such as



(a) An IKS with configuration mentioned as FUT



(b) An IKS with configuration mentioned as FDB

**Figure 6.** Two IKS of CRX-10ia/L at a pose with different configurations as presented by the ROBOGUIDE® software.

unreachable poses in the path, singularities, joint limits, and internal collisions. It is important to note that if a path is infeasible for such a robot, it is not possible to change the IKS that can execute the desired path without crossing a singularity. A feasible closed path for noncuspidal robots is always repeatable as the robots do not undergo a nonsingular change of solutions, and thus path feasibility implies path repeatability. This is not true for cuspidal robots, and the path feasibility is dependent upon the initial IKS Wenger (2004). As cuspidal robots can undergo a nonsingular change of solutions while performing a closed path, a feasible path may not necessarily be repeatable. An example of a feasible but non-repeatable path in a commercial cuspidal robot was discussed in Salunkhe et al. (2023). For an open path, the feasibility is dependent on the initial IKS and the possibility of changing the IKS before executing the path. The case of changing IKS and making an infeasible path feasible is of prime importance in commercial cuspidal robots that are used in collaborative tasks. A time optimal trajectory planning algorithm that considers nonsingular change of solutions is presented in Marauli et al. (2023). The complete classification of possible paths for a cuspidal robot is presented in Figure 7 and Figure 8.

If the path is a closed loop in the workspace, then we have further classification of feasible paths depending on their repeatability. A repeatable path can either correspond to a regular path (see Section 3) or a nonsingular change

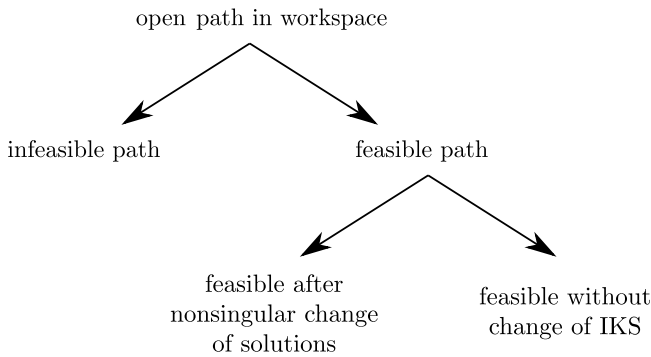


**Figure 7.** The classification of possible open paths in cuspidal robots.

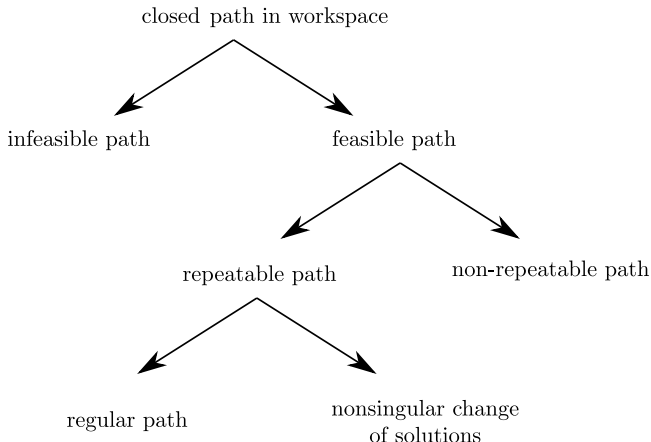


**Figure 8.** The classification of possible closed paths in cuspidal robots.

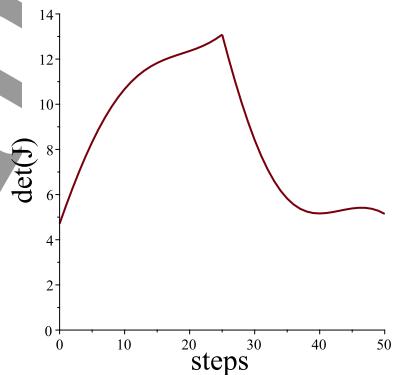
of solutions. We consider two closed paths in two different cuspidal robots to illustrate the different types of paths in a cuspidal robot. Figure 11 shows a closed path in a 2D slice of the workspace of the Jaco robot (refer to Figure 9). Figure 11b shows the  $\theta_1$  value of each IKS along the path.



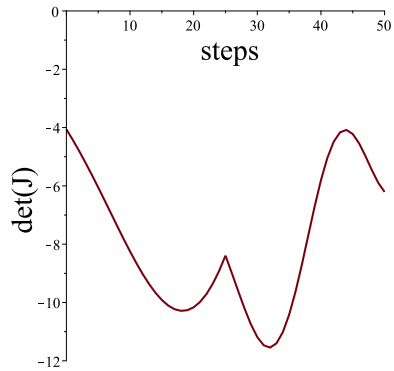
**Figure 9.** Jaco Gen 2 robot from Kinova robotics.  
(Source: <https://www.kinovarobotics.com/product/gen2-robots>)

As the path is a closed loop, the IKS at the beginning of the path should match the final IKS. In Figure 11, the top side is considered to be glued to the bottom side as  $\theta_1$  is equal modulo  $2\pi$ . The right side is to be glued to the left side as the path is a closed path and the final EE-pose of the path is equal to the EE-pose at the start of the path. As there are eight IKS for the starting pose of the trajectory, there

are eight possible trajectories, denoted as  $T_i, i \in \{1..8\}$ . The blue color paths are the solutions in an aspect with  $\det(\mathbf{J}) > 0$  while the red paths correspond to  $\det(\mathbf{J}) < 0$ . This path example has been treated in detail by Salunkhe et al. (2023), and it was shown that the 8 IKS belong to two separate aspects such that a nonsingular change of solutions can be performed between any two IKS corresponding to blue (resp. red) paths. An example of nonsingular change of solutions between two IKS in aspects with  $\det(\mathbf{J}) > 0$  (resp.  $< 0$ ) is shown in Figure 10a (resp. 10b). The path in the joint space shown in Figure 10a is a linear interpolation between  $\mathbf{q}_1 = [-2.89, -0.41, 2.61, -2.79, 3.03, -0.33]$  and  $\mathbf{q}_2 = [3.01, -0.42, 2.43, 0.53, 3.01, 2.25]$  via  $[0, -0.39, 2.76, -1.11, 2.50, 0]$ . The path in the joint space in Figure 10b is a linear interpolation between  $\mathbf{q}_3 = [-2.89, -0.42, 2.44, 2.75, -3.04, 0.28]$  and  $\mathbf{q}_4 = [3.00, -0.42, 2.65, -0.44, -2.98, 3.05]$  via  $[0, -1.47, 3.49, 2.95, -2.74, 0]$ . The vectors  $\mathbf{q}_{1..4}$  are the IKS of the EE-pose corresponding to the start of the closed path shown in Figure 11a.



(a) Nonsingular change of solutions in aspect with  $\det(\mathbf{J}) \geq 0$ .



(b) Nonsingular change of solutions in aspect with  $\det(\mathbf{J}) \leq 0$ .

**Figure 10.** The  $\det(\mathbf{J})$  plot against the discrete path in the joint space from one IKS to another IKS of the ee-pose corresponding to a in Figure 11a

Among the eight paths in Figure 11b,  $T_2$  and  $T_6$  are continuous paths with the same initial and final IKS. These paths are regular closed paths. Due to their discontinuity  $T_3, T_4, T_7$  or  $T_8$  are infeasible paths. The paths  $T_1$  and  $T_5$  are continuous but not repeatable since the initial and final IKS are not equal. In such cases, the path is continuous and can be traversed once but can not be repeated as the final IKS corresponds to an initial IKS that leads to an infeasible path (i.e. traversing  $T_1$  will lead to traversing  $T_8$  if the path

would be repeated). It is worth noting that no repeatable path without crossing singularity is possible when the robots start a path from an IKS belonging to the red paths i.e.  $T_1, T_4, T_5, T_8$ . On the other hand in Innocenti and Parenti-Castelli (1998) continuous repeatable paths with different initial and terminal IKS were discussed. Figure 12 shows an example from Innocenti and Parenti-Castelli (1998) of such paths denoted with  $\bar{T}_1$  and  $\bar{T}_2$ . These paths describe a nonsingular change of IKS that is continuous and repeatable i.e. the terminal IKS of  $\bar{T}_1$  is the initial IKS of  $\bar{T}_2$ . These examples are illustrated in Extension 1.

### 4.3 Types of scenarios

As discussed in the previous section, there exist more types of paths in a cuspidal robot than in a noncuspidal robot. The direct implication of this fact is that we also encounter different scenarios in the path planning. The scenarios relevant for industrial applications are pick and place operations, repetitive tasks forming a closed path (e.g. welding, surface inspection), or point-to-point trajectories. We will discuss path planning in the workspace only as the paths in the joint space are simpler and can cross singularities without issues. The different scenarios in cuspidal robots are illustrated in Figure 13 and 14.

*Scenarios in closed paths:* These scenarios are often encountered in welding or inspection applications. The robot is expected to follow a given path in the workspace and return to its initial pose. Such paths can be repetitive like welding in an assembly line or can be one-time tasks such as inspecting a unique part. In the case of nonrepetitive tasks, a path leading to a nonsingular change of solutions is acceptable while the repetitive tasks should be regular paths to be declared as feasible. In special cases where the nonsingular change of solutions is repeatable, such paths can be declared suitable for repetitive tasks but may face issues such as collisions with the environment. For this reason, a path specified in the workspace has to be analyzed for the intersection with critical values. If the path does not cross critical values, it is a regular path. In case the path intersects the critical values, it is important to verify the initial IKS as well as compare it with the final IKS. An example of a closed loop path crossing critical values is shown in Figure 11. It is observed that to complete the closed path, it is important to start the path from the IKS corresponding to either  $T_1, T_2, T_5$  or  $T_6$ . Furthermore, if the task is repetitive then IKS belonging to  $T_1$  and  $T_5$  are to be discarded. It is clear from this illustration that for a given path to be declared feasible, the choice of initial IKS plays a crucial role in cuspidal robots.

*Scenarios in open paths:* These scenarios are simpler than the closed loop paths. A typical example of this scenario is an open path of welding that starts at a point and terminates at another point. In such a case the robot is not expected to return to its initial pose. In case the path does not cross critical values, it is always feasible. The feasibility of the paths that cross the critical values depends on the choice of initial IKS. In the example path shown in Figure 11a, the paths  $a \rightarrow b$ ,  $b \rightarrow c$ ,  $c \rightarrow d$  and  $d \rightarrow a$  can be considered as open paths individually. The paths  $b \rightarrow c$  and  $c \rightarrow d$  do not cross any critical values. In  $b$  (resp.  $c$ ), thus, any IKS can be chosen to reach  $c$  (resp.  $d$ ). This is clear from the

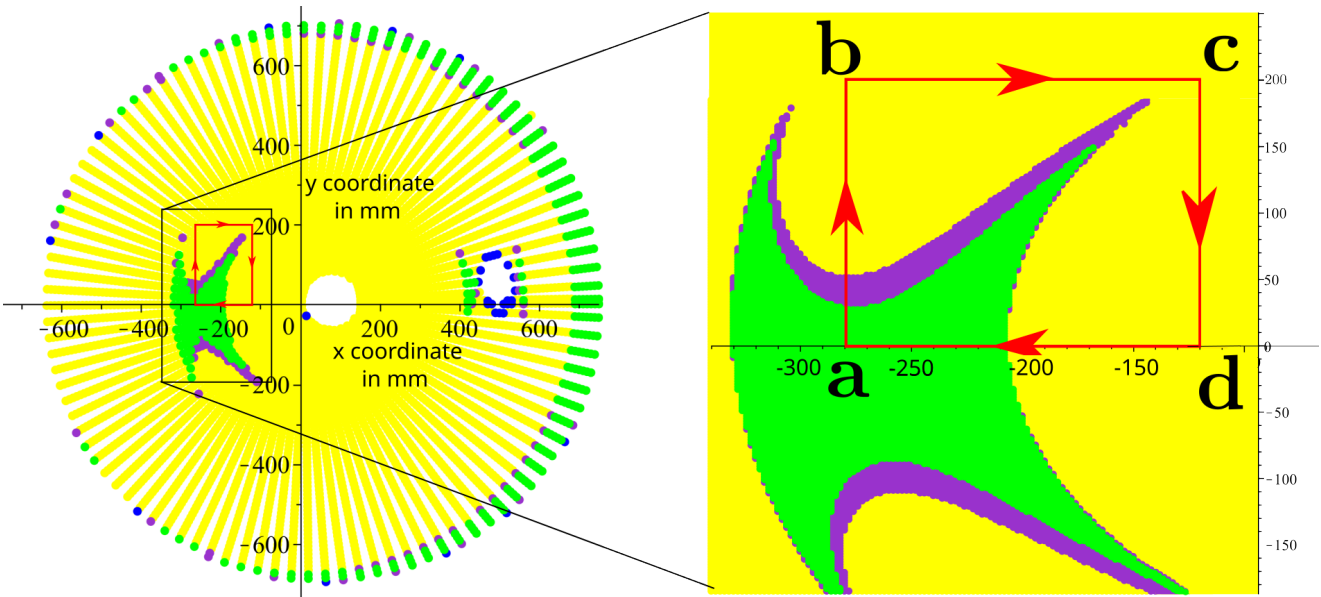
parts between the dotted lines annotated as  $b$ ,  $c$  and  $d$  in Figure 11b. But, for paths  $a \rightarrow b$  and  $d \rightarrow a$ , the choice of initial IKS is important. It is observed in Salunkhe et al. (2023) that the choice of good initial IKS is dependent on which boundary of the region with 8 IKS is crossed. These boundaries of a region with 8 IKS (green color region in Figure 11a) in the workspace are examples of components of critical values. A continuous path in the workspace of a cuspidal robot is not guaranteed if it crosses two distinct components of critical values Wenger (2004); Salunkhe et al. (2022b).

### 4.4 Path planning framework

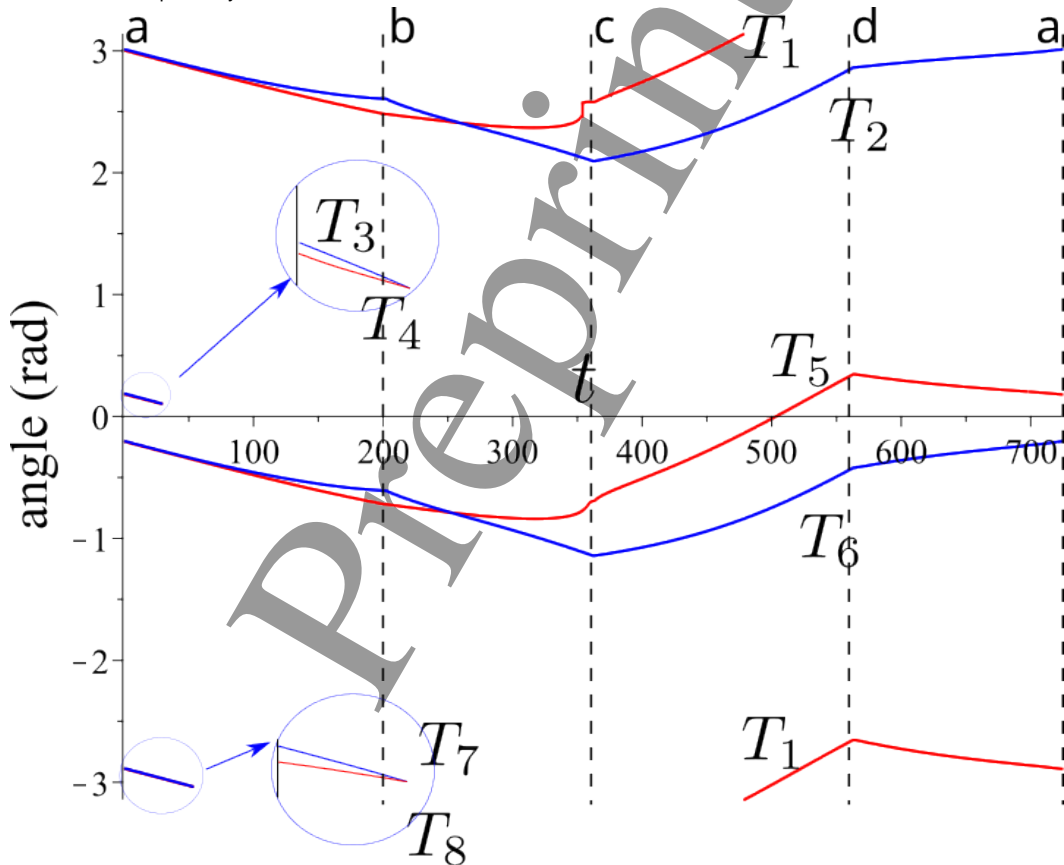
Based on the types of paths and scenarios in cuspidal robots as shown in previous subsections, we propose a path-planning algorithm for cuspidal robots. This algorithm addresses all the scenarios discussed in the previous subsection. The algorithm proposed can be implemented in existing commercial cuspidal robots such as the Jaco Gen2 robot from Kinova Robotics, and the CRX series from FANUC. The algorithm is divided into two parts; the first part deals with the open paths in the workspace and the second part with the scenarios related to closed-loop paths in the workspace.

*Algorithm for open paths:* The flowchart in Figure 15 explains the algorithm to be used in case of open paths for a cuspidal robot. The main consideration in such cases is the intersection of the path with the critical values. In case the path intersects the critical values, we can verify the connectivity of the path starting from every IKS of the initial pose of the path. It is known that the number of IKS either increases or decreases upon crossing a critical value and traveling from a region with a lower number of IKS is never a problem as we gain extra IKS. To this end, the path is evaluated at discrete values of the path parameter, i.e. an equidistant discretization of  $t \in [0, 1]$ , which results in a finite number of EE-poses. At each of these EE-poses, the IKS is computed using an appropriate algorithm (e.g. HuPf algorithm Husty et al. (2007)). We then propose to choose an EE-pose along the path that corresponds to a region with the least number of IKS. The connectivity of every IKS of this EE-pose with a chosen initial IKS (at the beginning of the path) is investigated. In case an IKS is connected, the forward connectivity of the IKS (at the chosen EE-pose) with the final IKS (at the end of the path) is investigated. If an IKS is connected to both the initial as well as final IKS, then such a path is declared as feasible. After repeating the connectivity check of every IKS of the selected EE-pose with the IKS of the initial EE-pose as well as the IKS of the final EE-pose, the feasible paths can be further optimized for execution.

*Algorithm for closed paths:* The flowchart in Figure 16 explains the algorithm to be adapted in case of closed paths for a cuspidal robot. This case presents more scenarios and the choices are complicated. As already shown, a given closed path can be continuous and yet not repeatable. The main consideration in such cases is whether a nonsingular change of solutions is acceptable for declaring a path feasible. The continuity of a path can be checked in the



(a) A closed loop path crossing multiple connected regions in the workspace of the Jaco robot. The yellow, purple, and green colors denote the regions with 4, 6, and 8 IKS respectively.



(b) Value of  $\theta_1$  along the closed path in Figure 11a, with regions of 4, 6 and 8 IKS. Blue and red paths correspond to solutions in an aspect with  $\det(\mathbf{J}) > 0$  and  $\det(\mathbf{J}) < 0$  respectively.

**Figure 11.** A closed loop path in the workspace of the commercial cuspidal robot Jaco Gen2, and the evolution of  $\theta_1$  along the path from Salunkhe et al. (2023) (see Extension 1).

same manner as discussed in the algorithm for open paths. A connected path is not enough to declare the feasibility and the type of task should be known beforehand to optimize and execute a given closed path in the workspace. This algorithm accounts for all the cases that can occur in commercial robots.

The types of paths, the different scenarios, and the algorithm proposed for path planning in cuspidal robots suggest that the complete path to be followed should be known before execution. This implies that cuspidal robots are NOT suitable for tasks where the path to be followed depends on the agent acting on the robot. In such tasks, the

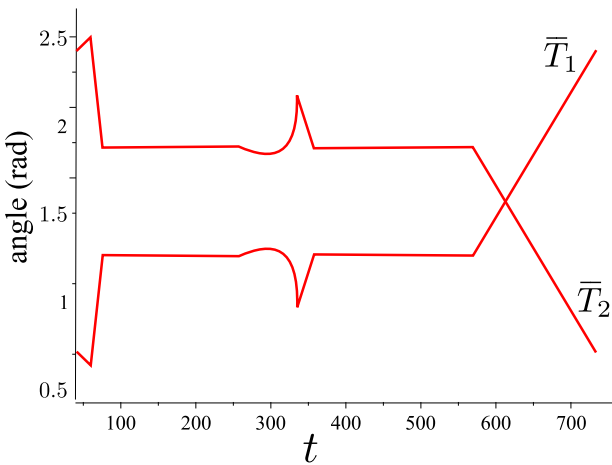


**Figure 12.**  $\theta_2$  value along the repeatable path that corresponds to a nonsingular change of solution (path mentioned in Innocenti and Parenti-Castelli (1998)).

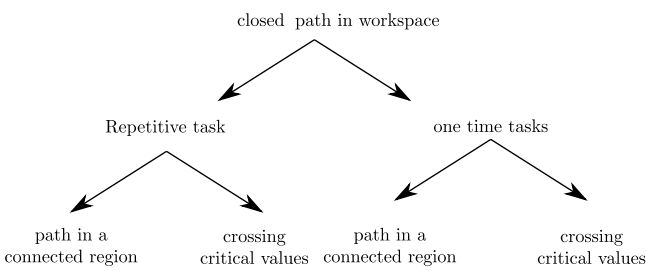


**Figure 13.** The classification of possible scenarios of closed paths in cuspidal robots.

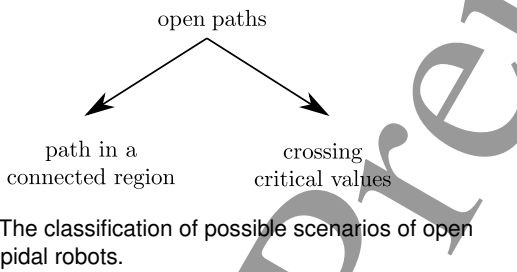


**Figure 14.** The classification of possible scenarios of open paths in cuspidal robots.

interaction is unpredictable, and the path is calculated in real-time. This is an important observation and a key contribution of the paper as almost all the commercial cuspidal robots that exist in the industry exist under the category of collaborative robots or 'cobots'.

## 5 Deciding cuspidality

In this section, we discuss the limitations of existing methods in deciding cuspidality and propose a generic method that can be applied to all 6R robots and incorporate the joint limits and collision constraints too. This method is easy to implement and is faster than the certified algorithm Chablat et al. (2022) in the case of a cuspidal robot. We propose a complete algorithm that can be used for deciding the cuspidality of a 6R robot. It combines all the previously known results as well as considers the analysis of the determinant of Jacobian to accelerate the decision time.

### 5.1 Effect of constraints on cuspidality analysis

The definition of cuspidality and the necessary and sufficient condition for cuspidality in a 3R robot discussed in Salunkhe et al. (2022b) is valid without the consideration of joint limits and collision constraints. Figure 17 shows an example of a 3R robot where we implement joint limits such that the cusp points in the workspace are inaccessible and yet there exists a nonsingular change of solutions. This qualifies the robot as cuspidal without encircling a cusp point. Even though such joint limits are virtual as they are bound externally, it is helpful to note that the cuspidality analysis should extend beyond checking the necessary and sufficient condition only. The certified algorithm proposed in Chablat et al. (2022) can incorporate the joint limits as long as the constraints are expressed algebraically. Another important constraint that affects the workspace and cuspidal behavior of a 6R robot is the collisions of different links of the robot. The internal collision between links limits the workspace of a robot to a great extent and this impacts the cuspidality analysis. The necessary and sufficient condition as well as the certified algorithm proposed fail to incorporate the collision constraint. The constraints are neither smooth nor algebraically expressible which makes them hard to incorporate in the certified algorithm.

### 5.2 Algorithm for deciding cuspidality

In this section, we propose an algorithm that is capable of deciding the cuspidality of a robot by incorporating both, joint limits as well as internal link collision constraints.

**5.2.1 6R robots with simplified architectures** The results for cuspidality from 3R robots can be extended to the wrist-partitioned 6R robots Wenger and Chablat (2022), where the wrist is formed by the last three joints. This is attributed to the reason that the position and orientation of such robots are decoupled. The wrist singularity in such robots is well known and the solutions for the orientation are always separated by wrist singularity. This makes the wrist a noncuspidal robot and so the cuspidal nature of the complete 6R robot depends on the cuspidal nature of the 3R robot formed by the first three axes only. The necessary and sufficient condition derived for a generic 3R robot used the geometric interpretation of the IKM for the proof. It is shown in Pieper (1968) that this geometric interpretation holds even for wrist-partitioned robots if the wrist kinematics is formed by the first three joints. This suggests that all the theorems proved for a generic 3R robot can be extended to wrist-partitioned 6R robots with a wrist at the end or the beginning of the robot. Apart from the above results, it is also known that the UR5 robot is noncuspidal Capco et al. (2020) with eight solutions in eight aspects. In the next section, we present the importance of analyzing the determinant of the Jacobian matrix and present new conditions for a robot to be noncuspidal.

**5.2.2 Determinant analysis** As the number of aspects are governed by the singularities in the joint space, it is of high importance that we study the determinant of the Jacobian matrix of a generic 6R robot. A simplified determinant for a 6R robot can be derived symbolically by using the

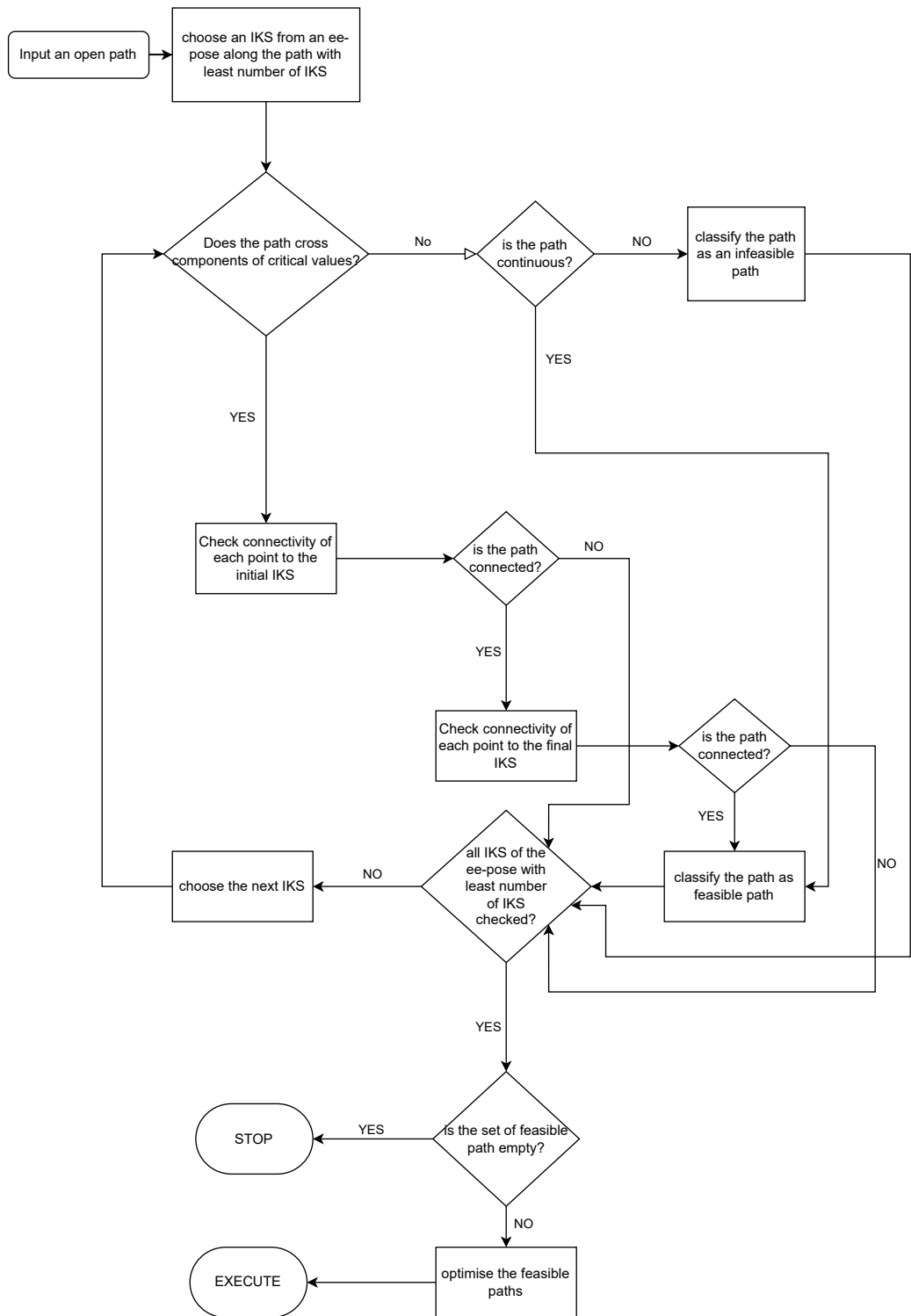


**Figure 15.** Path planning algorithm for scenarios with open paths in cuspidal robots.

preferential Jacobian as mentioned in Gorla and Renaud (1984) and Khalil and Dombre (2004). The analysis of the factors of the determinant of the Jacobian plays a fundamental role in orthogonal 3R robots. We discuss an example of anthropomorphic architecture with a wrist at the end. To analyze this example, we substitute D-H parameters

$$a_3 = a_4 = a_5 = d_5 = \alpha_2 = 0. \text{ The } \det(\mathbf{J}) \text{ of such a robot is}$$

$$\det(\mathbf{J}) = C \cos(\theta_3) \sin(\theta_5) (\sin(\alpha_3)d_4 \sin(\theta_2 + \theta_3) + a_2 \cos(\theta_2) + a_1) \quad (7)$$

where  $C = a_2 d_4 \sin(\alpha_1) \sin(\alpha_3) \sin(\alpha_4) \sin(\alpha_5)$  is a constant. As the determinant factors in three components, it is readily seen that there exist at least eight aspects in the joint space of such a robot. These aspects arise due to the transversal intersection of the components that produce at

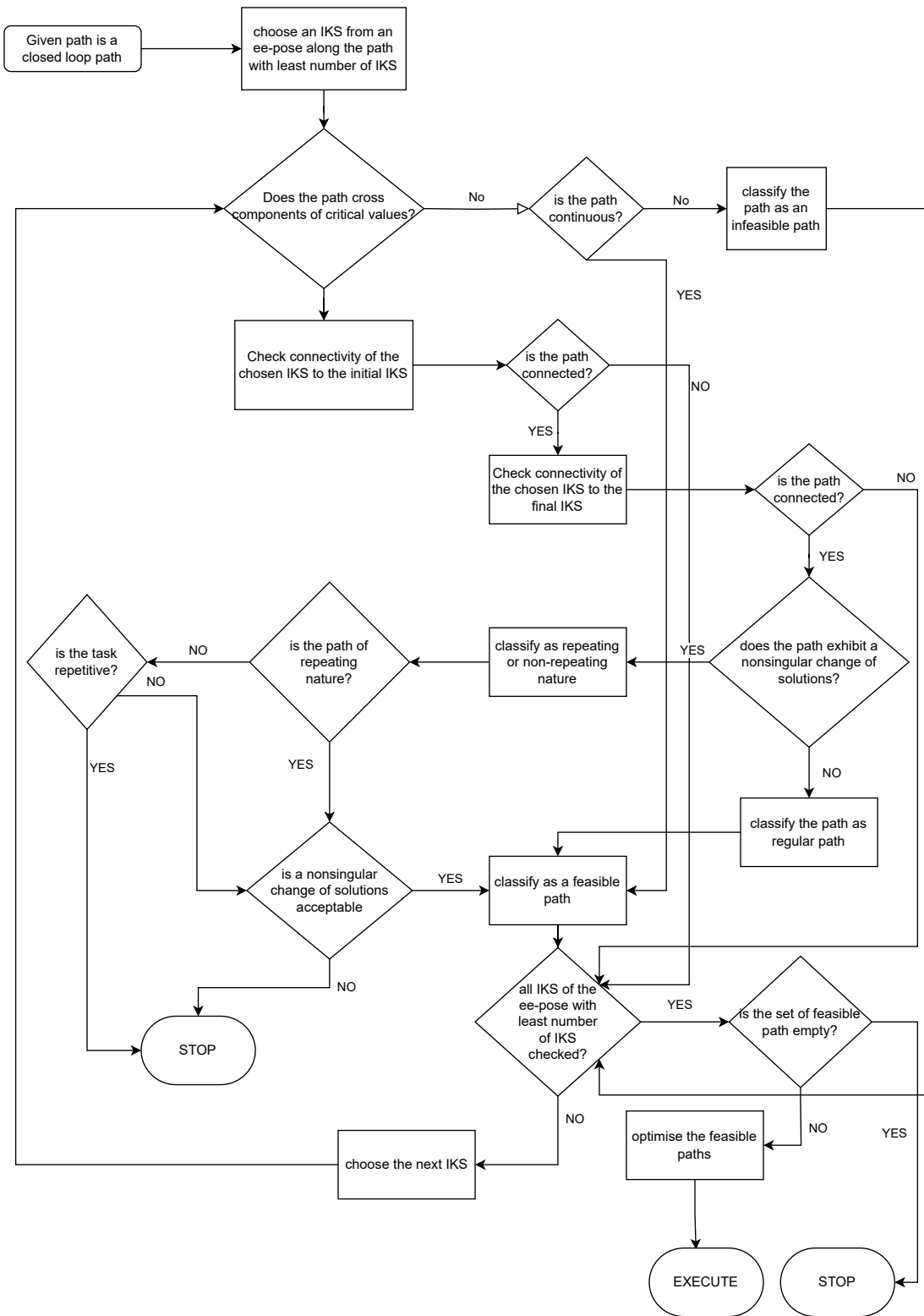


**Figure 16.** Path planning algorithm for scenarios with closed-loop paths in cuspidal robots.

least two aspects each. Upon geometric analysis of IKM, it can be shown that the components  $\cos \theta_3$  and  $\sin \theta_5$  give four IKS separated by singularities. They determine the elbow (up/down) and wrist (flip/unflip) configurations respectively. The third component produces two aspects, and thus the eight IKS of such architecture are always separated by singularities.

A similar argument shows that the determinant of a UR5

robot takes the following form

$$\begin{aligned}
 \det(\mathbf{J}) = & 9097 \sin(\theta_5) \sin(\theta_3) (1707 \cos(\theta_2) \sin(\theta_3) \\
 & \cos(\theta_4) + 1707 \cos(\theta_2) \sin(\theta_4) \cos(\theta_3) \\
 & - 1707 \sin(\theta_2) \sin(\theta_3) \sin(\theta_4) + \\
 & 1707 \sin(\theta_2) \cos(\theta_4) \cos(\theta_3) - \\
 & 4265 \cos(\theta_2) \cos(\theta_3) + 4265 \sin(\theta_2) \\
 & \sin(\theta_3) - 4873 \cos(\theta_2))
 \end{aligned} \tag{8}$$

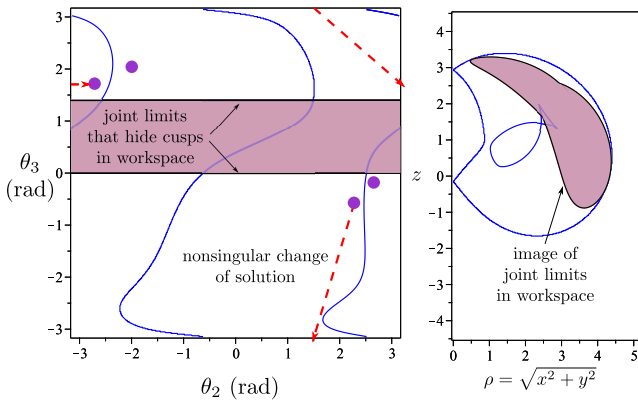


**Figure 17.** Nonsingular change of solutions in 3R cuspidal robot with joint limits hiding the cusp points. Robot parameters:  $\mathbf{d} = [0, 1, 0]$ ,  $\mathbf{a} = [0.8, 1.7, 1.8]$ ,  $\alpha = [\frac{\pi}{6}, \frac{\pi}{3}, 0]$ .

If the determinant factors into at least three components, the number of aspects is at least eight and the geometric analysis of IKM may be able to conclude on cuspidality. This leads to the following question: Can we identify 6R robots with simplified architectures such that the  $\det(\mathbf{J})$  is factored in at least three factors? The  $\det(\mathbf{J})$  is a function of in total of 14 D-H parameters that define the architecture of the robot. These 14 parameters are  $d_{2..5}$ ,  $a_{1..5}$ ,  $\alpha_{1..5}$ , and the classification space is huge. The identification can be simplified by providing two values for each parameter. If the parameter is a length parameter, i.e.  $d_i$  or  $a_i$ , then it can be either 0 or a symbolic value. For the axes alignment, only orthogonal ( $\alpha_i = \frac{\pi}{2}$  radians) and parallel ( $\alpha_i = 0$  radians) arrangements were considered. This analysis investigates the number of components of the  $\det(\mathbf{J})$  obtained from the preferential Jacobian. The total types of robots investigated are  $2^{14} = 16384$ , and 832 types of robots (~5%) were found to be of simplified architecture. The D-H parameters of some of these robots are mentioned in Appendix B. The symbolic values of the length parameters can take any nonzero value and the robot preserves the factored form of robots. This result is a doorway for designers to investigate new designs that are noncuspidal and may have advantages in specific cases. The orthogonal robots have been shown to exhibit better dynamic properties compared with the anthropomorphic architectures Nguyen et al. (2012), and it will be interesting to explore different noncuspidal designs with simplified IKM.

**5.2.3 Generic case of 6R robot** An algorithm that considers joint limits and collision constraints to decide upon the cuspidality of a 6R robot is important for real-life applications. Thus, a practical algorithm, similar to Marauli et al. (2023), based on solving an optimal-path-planning (OPP) problem is proposed. To decide cuspidity, the OPP problem has to be solved for the whole workspace until a connection of at least two IKS is found. Since checking the whole workspace using numerical approaches is computationally demanding, it is discretized into a finite  $n_W$  points  $\mathbf{x}_k \in \mathcal{W}$ ,  $k \in \{1 \dots n_W\}$ . The discretized workspace impacts the decision on cuspidity, which is discussed in more detail when explaining the algorithm.

The connectivity problem consists of finding a nonsingular path between two different IKS  $(\mathbf{q}_i, \mathbf{q}_j) \in \mathcal{I}_{\mathbf{x}}$ . Therefore,

a measure of distance to the singularity is required. In the literature various methods to measure the distance exist, such as the kinematic manipulability Doty et al. (1995), condition number, smallest eigenvalue, or determinant of the Jacobian to name a few. We use  $\det(\mathbf{J})$  since it plays an important role in cuspidity analysis.

**Optimal-Path-Planning problem:** Given an initial IKS  $\mathbf{q}_0 \in \mathcal{I}_{\mathbf{x}}$  to an arbitrary EE-pose  $\mathbf{x}$ . Find a nonsingular path  $\mathbf{q}(t)$  connecting  $\mathbf{q}_0$  with a valid IKS  $\mathbf{q}_1 \in \mathcal{R}_{\mathbf{q}_0, \mathbf{x}}$ . The goal is to find a path as far as possible to any singularity. Therefore, the smallest value of the determinant along the path

$$\inf_t \text{sign}(\det \mathbf{J}(\mathbf{q}_0)) \det \mathbf{J}(\mathbf{q}(t)) \quad (9)$$

is maximized. The multiplication with the sign of the initial determinant enables the use of the function  $\inf$  also for negative values i.e.  $\det \mathbf{J}(\mathbf{q}_0) < 0$ . A negative value of (9) results in an invalid solution since condition (5) is not met. As smooth joint paths  $\mathbf{q}(t)$  are desirable, an integrator chain represented by  $\mathbf{z}' = \mathbf{f}(\mathbf{z}, \mathbf{u}, t)$ , with states

$$\mathbf{z}^T = [\mathbf{q}^T, (\mathbf{q}')^T, (\mathbf{q}'')^T]$$

and input  $\mathbf{u} = \mathbf{q}'''$  are used to receive a three times differentiable path. The derivative with respect to the path parameter  $t$  is denoted as  $(') = \partial() / \partial t$ . The OPP problem is then written as a nonlinear optimization problem

$$\begin{aligned} & \max_{\mathbf{z}, \mathbf{u}} \left( \inf_t \text{sign}(\det \mathbf{J}(\mathbf{q}_0)) \det \mathbf{J}(\mathbf{q}(t)) \right), \\ & \text{s.t. } \mathbf{z}' = \mathbf{f}(\mathbf{z}, \mathbf{u}, t), \quad \mathbf{q}(0) = \mathbf{q}_0, \quad \mathbf{q}(1) = \mathbf{q}_1, \\ & \quad \underline{\mathbf{z}} \leq \mathbf{z}(t) \leq \bar{\mathbf{z}}, \quad \underline{\mathbf{u}} \leq \mathbf{u}(t) \leq \bar{\mathbf{u}}, \\ & \quad \text{for } t \in [0, 1]. \end{aligned} \quad (10)$$

The geometric lower and upper bounds are denoted by  $(\underline{})$  and  $(\bar{})$ . These bounds can be used to incorporate joint limits and influence the geometric derivatives. The OPP problem is solved with a multiple shooting approach Bock and Plitt (1984) implemented in MATLAB 2020 using CasADI Andersson et al. (2019) and Ipopt Wächter and Biegler (2006) as solver. It is worth noting that the value of the objective function can be negative exactly at the optimal point.

**The Algorithm:** The OPP problem is solved for all discrete EE-poses  $\mathbf{x}_k$ ,  $k \in \{1 \dots n_W\}$ , until a connection between two distinct IKS is found. To this end, the optimization problem (10) is solved for a given initial and terminal IKS  $\mathbf{q}_0 \in \mathcal{I}_{\mathbf{x}}$ ,  $\mathbf{q}_1 \in \mathcal{R}_{\mathbf{q}_0, \mathbf{x}}$  of a chosen EE-pose e.g.  $\mathbf{x}_0$ . If a feasible solution is found (i.e. positive value of the objective) the connectivity problem is solved and the robot is cuspidal. If the optimization is unsuccessful, a different terminal IKS  $\mathbf{q}_1 \in \mathcal{R}_{\mathbf{q}_0, \mathbf{x}}$  of the same EE-pose  $\mathbf{x}_0$  is chosen and the problem is solved again. If no connection could be found e.g.  $\mathbf{x}_0$ , then a different EE-pose  $\mathbf{x}_k, k \neq 0$ , is picked and the procedure is repeated. In the case that all grid points  $\mathbf{x}_k$  are checked unsuccessfully no assertion about cuspidity can be made. It is worth noting, that a grid refinement of the workspace (or a different grid) can lead to a reliable check of cuspidity since only a finite number of points in the workspace are considered in the procedure. Algorithm 1 details the implementation.

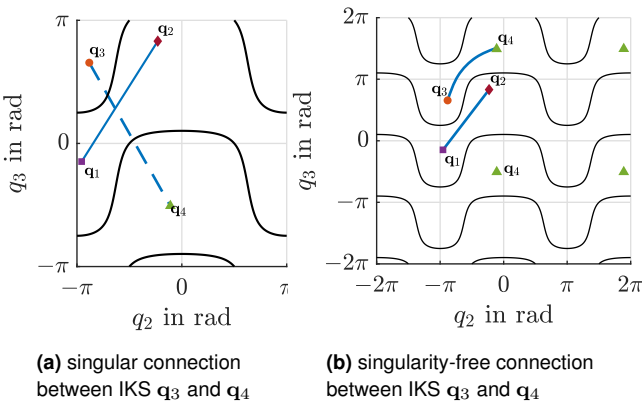


**Figure 18.** Example for considering clockwise and counterclockwise rotations in the IKS.

#### Algorithm 1 Proposed cuspidality deciding algorithm.

**Require:** Discretized workspace EE-poses  $\{x_1 \dots x_{n_w}\}$

```

for all  $k \in \{1..n_w\}$  do
    - compute IKS and pick initial  $q_0 \in \mathcal{I}_{x_k}$ 
    for all  $q_1 \in \mathcal{R}_{q_0, x_k}$  and  $q_1 \neq q_0$  do
        - solve OPP problem (10)
        if successful then
            - connectivity found  $\Rightarrow$  break
    if connectivity found then
        - robot is cuspidal
    else
        - no assertion about cuspidality possible

```

*Numerical aspects:* Algorithm 1 takes care of numerical difficulties encountered by the fact that different revolute joint angles are equal modulo  $2\pi$ . Since these joints can rotate freely, clockwise as well as counterclockwise rotations must be taken into account. The joint coordinates are defined by a  $n$ -torus  $\mathbb{T}^n$ . Therefore, adding  $\pm 2k\pi$  with  $k \in \mathbb{N}_0$  does not change the IKS, i.e.  $x = f(q) = f(q \pm 2k\pi)$ . For practical applications, only solutions within the interval  $q \in [-2\pi, 2\pi]$  have to be considered. Consider planning singularity-free trajectories for a 3R robot (D-H parameters in Figure 1) connecting the IKS in one aspect, as shown in Figure 18a. A nonsingular trajectory between  $q_1$  and  $q_2$  is readily found. On the other hand, planning a trajectory between  $q_3$  and  $q_4$  without crossing a singularity is not possible, since the OPP problem (10) does not consider the periodicity of the joint coordinates. Extending the solution space of  $q_4$  to the interval  $[-2\pi, 2\pi]$ , i.e. adding multiple of  $\pm 2\pi$  element-wise, enables connecting the IKS  $q_3$  and  $q_4$  without crossing a singularity as shown in Figure 18b. This results in a counterclockwise rotation of the third joint.

The self-intersection of the set of singularities leads to a higher number of aspects and thus to a higher possibility of a noncuspidal robot. Such robots are of nongeneric type and it has been noted Pai and Leu (1992) that given a class of manipulators, almost all forward kinematic maps,  $f : \mathcal{J} \rightarrow \mathcal{W}$ , are generic and the nongeneric maps form a thin set of the class. Upon observation of the parameter space for 3R robots, it is not hard to expect that the neighborhood of a nongeneric design almost always leads to a cuspidal robot. This makes the practical algorithm very useful as the

nongeneric cases are identified with the determinant analysis, and the generic cases are analyzed by using the Algorithm 1. The algorithm is much faster than the certified algorithm presented in Chablat et al. (2022), if the robot is cuspidal. Solving IKS of a generic 6R robot with the HuPf algorithm takes an average of 10ms and the connectivity query required an average of 8.52 seconds (using PC with 32 Gb RAM and Intel i7 12<sup>th</sup> gen processor). In case all the points are to be investigated, the computation time depends on the resolution of the discretization. This case was never encountered as all the noncuspidal robots are already separated by using previously known results or the analysis of the determinant. The algorithm presented in Figure 19 can be automated to decide the cuspidality of almost all 6R robots. This algorithm will be inconclusive while analyzing those noncuspidal robots that neither have a  $\det(\mathbf{J})$  that factors in at least 3 components nor do any known results apply to the robot. We have analyzed 3240 robots with varying parameters for cuspidality, and the algorithm presented in Figure 19 was able to decide the cuspidal nature of each robot.

### 5.3 Application of the decision algorithm

In this section, we present the results obtained by implementing the deciding algorithm for cuspidality. The Algorithm 1 terminates with few iterations in the case of a cuspidal robot. The algorithm was able to decide about the cuspidal nature of every 6R robot that was given as an input. We have a 14-dimensional parameter space for cuspidality analysis which is not only huge but also impossible to visualize. We choose a specific 3-dimensional parameter space that includes the architecture of almost all types of known commercial robots, to highlight the importance of cuspidality analysis. Figure 20 shows the parameter space with  $d_5, \alpha_3$  and  $\alpha_4$  as the basis. All other D-H parameters for the robot are similar to those of the FANUC CRX-10ia/L robot. The cube was discretized into 3240 points and the robot corresponding to each point was analyzed for cuspidality. It was noted that every point inside the cube, i.e. not lying on the faces, corresponds to the D-H parameters of a cuspidal robot. The robots belonging to the face  $ABFE$  are degenerate as the  $\det(\mathbf{J})$  is always zero. The face  $ADHE$  corresponds to anthropomorphic architectures with the wrist at the end as  $d_5 = 0$ . It is a known result that the robots corresponding to the points on the face  $ADHE$  except the one at  $A$  are noncuspidal. The robot corresponding to  $A$  is a degenerate robot. The edge  $GH$  corresponds to the robots having anthropomorphic architecture with offset in the wrist. The robot corresponding to  $H$  is a wrist-partitioned anthropomorphic robot with an orthogonal wrist arrangement and thus noncuspidal. Every robot belonging to edge  $GH$  except the point  $H$  is a cuspidal robot, suggesting that the addition of an offset to the anthropomorphic architecture almost always leads to a cuspidal robot. The robots corresponding to face  $ABCD$  have a 3R subchain as  $\alpha_3 = 0$ . The edge  $CD$  corresponds to UR5 like architecture as  $\alpha_4 = \frac{\pi}{2}$ . Every robot belonging to the face  $ABCD$  except those lying on the edge  $AB$  (which corresponds to a degenerate robot) are noncuspidal as the  $\det(\mathbf{J})$  have three factors into three components and the robot has a simplified IKM that can be analyzed geometrically. The robots corresponding to face  $DCGH$

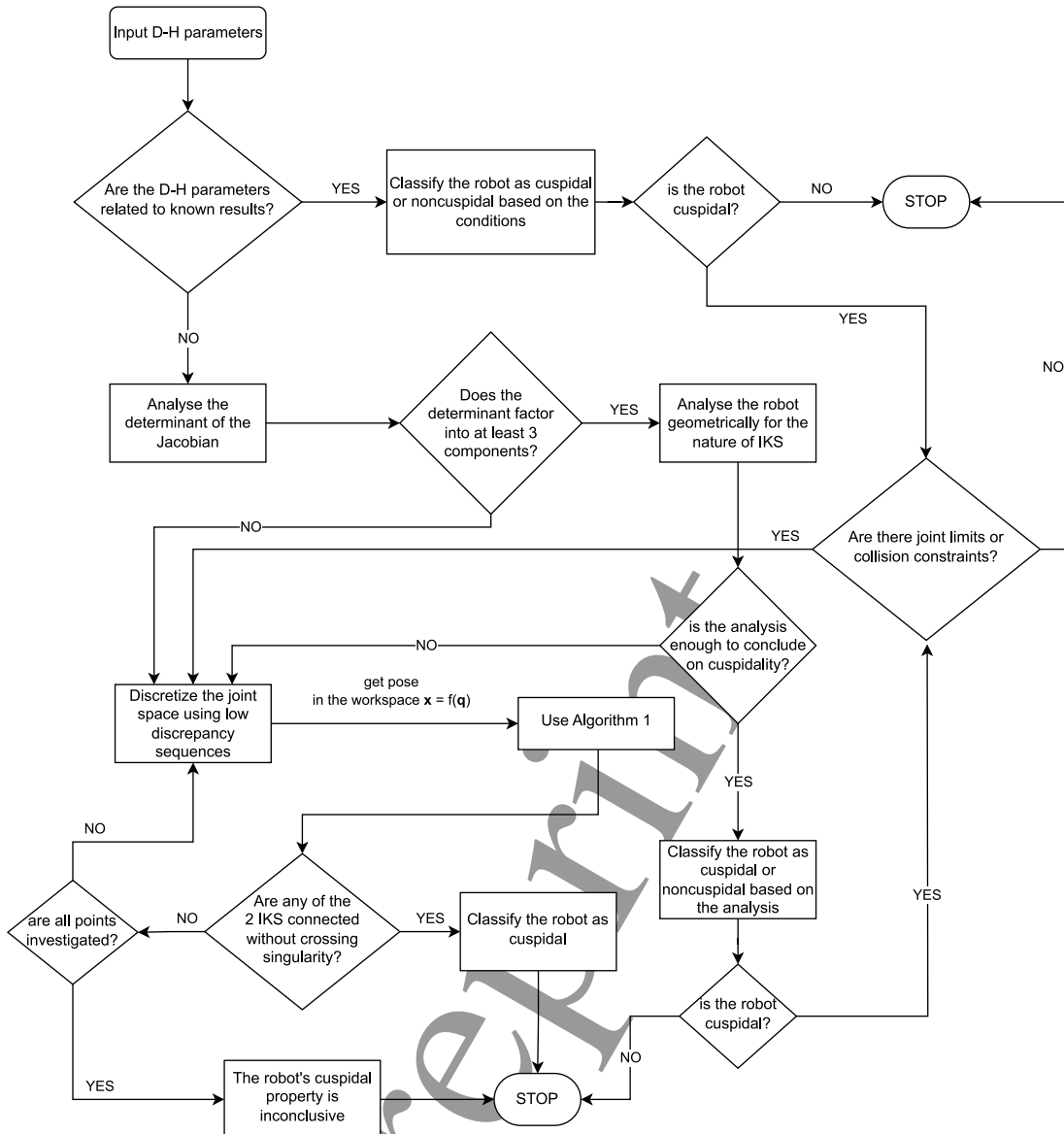


**Figure 19.** changesThe algorithm to decide if a given 6R robot is cuspidal or not.

except the edge  $CD$  and point  $H$  are cuspidal robots. These robots were found to be cuspidal by implementing Algorithm 1. The edge  $HE$  corresponds to wrist-partitioned robots with the nonorthogonal arrangement of the wrist. These robots are noncuspidal as the 3R positional subchain does not satisfy the necessary and sufficient condition to be cuspidal. The robots corresponding to the edge  $EF$  are degenerate. The face  $FGHE$  excluding edges  $GH$ ,  $HE$ , and  $EF$  corresponds to robots with an offset and a nonorthogonal arrangement of the last three joints. One such example of a commercial robot is the Jaco robot Gen2 (nonspherical wrist). These robots are found to be cuspidal by using the algorithm proposed in Figure 19. Similarly, all the robots on the face  $BCGF$  except  $B$ ,  $C$  and  $F$  were found to be cuspidal in nature. The robots corresponding to  $C$  are UR5 type robots for whom the  $\det(\mathbf{J})$  has three factors. This case corresponds to a noncuspidal robot. Robots corresponding to the face  $B$  and  $F$  are degenerate robots. It is concluded from these results that a robot with generic geometry is almost always a cuspidal robot. Extending the algorithm, some of the existing commercial robots are presented in table 1 with

the details on maximum IKS present in the workspace, and their cuspidal nature.

**Table 1.** Classification of some of the existing robots according to cuspidal nature.

Robot	Max IKS	Nature
ABB IRB 140, KUKA KR5	8	noncuspidal
UR5, UR10	8	noncuspidal
FANUC CRX-10ia/L	16	cuspidal
Kinova Link6	16	cuspidal
JACO Gen2 nonspherical wrist	12 <sup>‡</sup>	cuspidal

<sup>‡</sup>The maximum number of IKS found by searching the workspace with 100,000 points generated by a low discrepancy sequence.

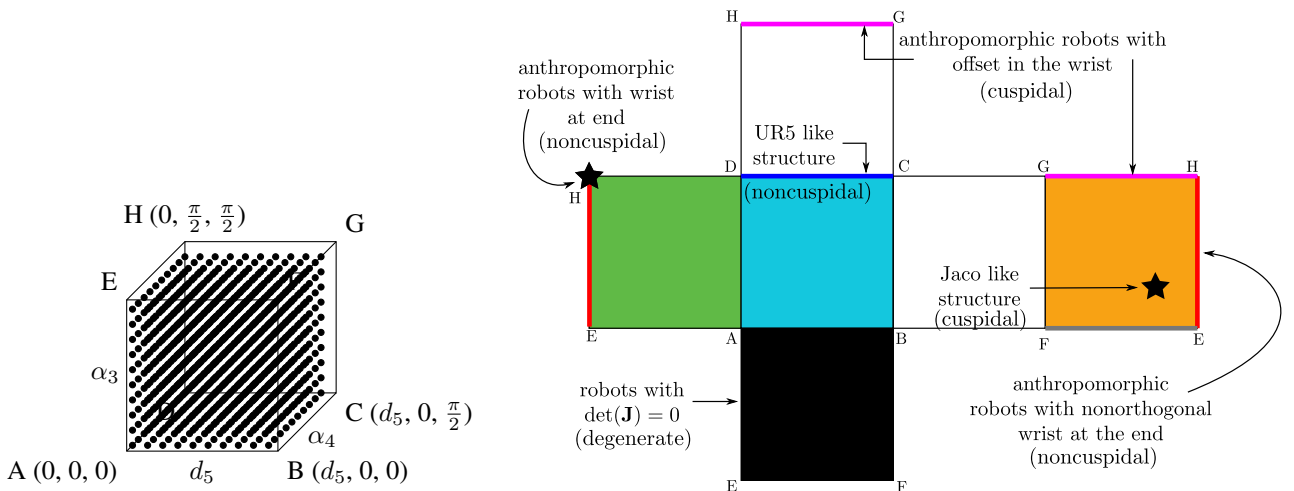


**Figure 20.** Classification of a 6R robot parameterized in specially chosen three D-H parameters. The rest of the DH parameters match that of the FANUC CRX-10ia/L robot.

## 6 Conclusions and Future work

In this work, the issues in path planning pertinent to cuspidal robots were discussed. The existing problems such as mislabeling of 'configurations', and incorrect calculations of IKS due to numerical methods were highlighted using deployed commercial cuspidal robots as examples. Later, the major kinematic issues such as the dependence of path feasibility as well as path repeatability on the choice of initial IKS were discussed. These issues prove to be dangerous in collaborative applications and the consequence of encountering a discontinuity in paths while crossing internal locus of critical values was discussed with examples in the workspace of an existing commercial cuspidal robot. Different scenarios possible in the path planning of cuspidal robots were presented highlighting the importance of considering cuspidality while designing path planning algorithms for robots. Though cuspidal robots can be used in industrial applications in a controlled environment, such robots are dangerous and cannot predict the feasibility of a path without complete knowledge of the path to be followed. We proposed a path-planning algorithm for cuspidal robots that considers different cases arising in cuspidal robots. The algorithm is capable of selecting good initial IKS that lead to feasible paths. In case of a bad initial IKS, the algorithm can suggest a possible nonsingular change of solution to be executed to make a given path feasible and repeatable. Considering the importance of deciding cuspidality for designing 6R robots, different decision methodologies of the past were presented. A practical algorithm was later presented to decide upon the cuspidal nature of 6R robots. The decision algorithm utilizes all the known results, exploits the form of  $\det(\mathbf{J})$ , and uses numerical approaches to decide upon the cuspidality of a generic 6R robot. This algorithm was implemented on thousands of generic architectures to further highlight that a generic design most likely leads to a cuspidal robot. To avoid designing a cuspidal robot, a few simplified architectures were presented whose determinant of the Jacobian factors into at least three components. This allows the designers to choose a new architecture from the catalog of noncuspidal robots with simplified IKM.

In the future, a dedicated package for the path planning of

6R robots will be deployed. This will implement algebraic approaches to solve for IKS and consider the cuspidal property of the robot. Interfaces that record both the joint angles as well as the EE-pose will be designed to replace the configurations classification of the IKS for cuspidal robots. Identification of cuspidal nature in robots with prismatic joints will be considered to extend the catalog of noncuspidal designs. As many cuspidal cobots are deployed in collaborative tasks, an algorithm that copes with unknown environments will be proposed using horizon planning. The new algorithm will be presented by using the presented work as its foundation.

## Acknowledgements

The authors are supported by the joint French and Austrian ECARP project: ANR-19-CE48-0015, FWF I4452-N.

## References

- Andersson JAE, Gillis J, Horn G, Rawlings JB and Diehl M (2019) CasADi - A software framework for nonlinear optimization and optimal control. *Mathematical Programming Computation*.
- Angerer A and Hofbaur MW (2013) Industrial versatility of inverse kinematics algorithms for general 6r manipulators. In: *16th International Conference on Advanced Robotics, ICAR 2013, 25-29 November 2013, Montevideo, Uruguay*. IEEE, pp. 1–7. DOI:10.1109/ICAR.2013.6766464.
- Baili M, Wenger P and Chablat D (2004) A classification of 3R orthogonal manipulators by the topology of their workspace. In: *IEEE International Conference on Robotics and Automation, 2004. Proceedings. ICRA '04. 2004*. New Orleans, LA, USA: IEEE, pp. 1933–1938 Vol.2.
- Bock H and Plitt K (1984) A multiple shooting algorithm for direct solution of optimal control problems\*. *IFAC Proceedings Volumes*.
- Borrel P and Liegeois A (1986) A study of multiple manipulator inverse kinematic solutions with applications to trajectory planning and workspace determination. In: *Proceedings. 1986 IEEE International Conference on Robotics and Automation*, volume 3. San Francisco, CA, USA: Institute of Electrical and Electronics Engineers, pp. 1180–1185.

- Burdick JW (1989) On the Inverse Kinematics of Redundant Manipulators: Characterization of the Self-Motion Manifolds. In: *1989 International Conference on Advanced Robotics*, volume 4. Ohio, p. 10.
- Capco J and Manongsong SM (2019) Implementing hupf algorithm for the inverse kinematics of general 6r/p manipulators. In: England M, Koepf W, Sadykov TM, Seiler WM and Vorozhtsov EV (eds.) *Computer Algebra in Scientific Computing*. Cham: Springer International Publishing. ISBN 978-3-030-26831-2, pp. 78–90.
- Capco J, Safey El Din M and Schicho J (2020) Robots, computer algebra and eight connected components. In: *ISSAC '20: International Symposium on Symbolic and Algebraic Computation*, ISSAC'20: Proceedings of the 45th International Symposium on Symbolic and Algebraic Computation. Kalamata / Virtual, Greece: ACM, pp. 62–69.
- Chablat D, Prébet R, Safey El Din M, Salunkhe DH and Wenger P (2022) Deciding cuspidality of manipulators through computer algebra and algorithms in real algebraic geometry. In: *Proceedings of the 2022 International Symposium on Symbolic and Algebraic Computation*, ISSAC '22. Villeneuve-d'Ascq, France: Association for Computing Machinery. ISBN 9781450386883, p. 439–448. DOI:10.1145/3476446.3535477.
- Denavit J and Hartenberg RS (1955) A Kinematic Notation for Lower-Pair Mechanisms Based on Matrices. *Journal of Applied Mechanics* 22(2): 215–221. DOI:10.1115/1.4011045. URL <https://doi.org/10.1115/1.4011045>.
- Doty KL, Melchiorri C, Schwartz EM and Bonivento C (1995) Robot manipulability. *IEEE Transactions on Robotics and Automation*.
- El Omri J and Wenger P (1995) How to recognize simply a non-singular posture changing 3-dof manipulator. In: *Proc. 7th Int. Conf. on Advanced Robotics*. pp. 215–222.
- Gorla B and Renaud M (1984) *Modèles des robots manipulateurs: application à leur commande*. Cepadues-Éditions.
- Gosselin C and Liu H (2014) Polynomial Inverse Kinematic Solution of the Jaco Robot. In: *International Design Engineering Technical Conferences and Computers and Information in Engineering Conference*, volume Volume 5B: 38th Mechanisms and Robotics Conference. p. V05BT08A055. DOI:10.1115/DETC2014-34152.
- Gutierrez A, Guda VK, Mugisha S, Chevallereau C and Chablat D (2022) Trajectory planning in dynamics environment: Application for haptic perception in safe human-robot interaction. In: Duffy VG (ed.) *Digital Human Modeling and Applications in Health, Safety, Ergonomics and Risk Management. Health, Operations Management, and Design*. Cham: Springer International Publishing. ISBN 978-3-031-06018-2, pp. 313–328.
- Husty ML, Pfurner M and Schröcker HP (2007) A new and efficient algorithm for the inverse kinematics of a general serial 6R manipulator. *Mechanism and Machine Theory* 42(1): 66–81. DOI:10.1016/j.mechmachtheory.2006.02.001.
- Innocenti C and Parenti-Castelli V (1998) Singularity-free evolution from one configuration to another in serial and fully-parallel manipulators. *ASME Journal of Mechanical Design* 120: 73–99.
- Khalil W and Dombre E (2004) *Modeling, Identification and Control of Robots*. New York: Springer. DOI:<https://doi.org/10.1016/B978-1-903996-66-9.X5000-3>.
- Kohli D and Spanos J (1985) Workspace Analysis of Mechanical Manipulators Using Polynomial Discriminants. *Journal of Mechanisms, Transmissions, and Automation in Design* 107(2): 209–215. DOI:10.1115/1.3258710.
- Marauli T, Salunkhe H Durgesh, Gatringer H, Mueller A, Chablat D and Wenger P (2023) Optimal motion planning for cuspidal manipulators: Application to commercial robots. In: *2023 IEEE/RSJ International Conference on Intelligent Robots and Systems*, Detroit, USA. p. 6.
- Nguyen DQ, Briot S and Wenger P (2012) Analysis of the dynamic performance of serial 3r orthogonal manipulators. In: *Volume 3: Advanced Composite Materials and Processing; Robotics; Information Management and PLM; Design Engineering, Engineering Systems Design and Analysis*. pp. 175–184. DOI: 10.1115/ESDA2012-82208.
- Paganelli D (2008) *Topological Analysis of Singularity Loci for Serial and Parallel Manipulators*. PhD Thesis, Universita di Bologna, Bologna, Italy.
- Pai D and Leu M (1992) Genericity and singularities of robot manipulators. *IEEE Transactions on Robotics and Automation* 8(5): 545–559.
- Pieper DL (1968) *The Kinematics of Manipulators Under Computer Control*. PhD Thesis, Stanford University, USA.
- Primrose E (1986) On the input-output equation of the general 7r-mechanism. *Mechanism and Machine Theory* 21(6): 509–510. DOI:[https://doi.org/10.1016/0094-114X\(86\)90134-5](https://doi.org/10.1016/0094-114X(86)90134-5).
- Salunkhe D, Capco J, Chablat D and Wenger P (2022a) Geometry based analysis of 3r serial robots. In: Altuzarra O and Kecskeméthy A (eds.) *Advances in Robot Kinematics 2022*. Cham: Springer International Publishing. ISBN 978-3-031-08140-8, pp. 65–72.
- Salunkhe DH, Chablat D and Wenger P (2023) Trajectory planning issues in cuspidal commercial robots. In: *2023 IEEE International Conference on Robotics and Automation (ICRA)*. pp. 7426–7432. DOI:10.1109/ICRA48891.2023.10161444.
- Salunkhe DH, Spartalis C, Capco J, Chablat D and Wenger P (2022b) Necessary and sufficient condition for a generic 3r serial manipulator to be cuspidal. *Mechanism and Machine Theory* 171: 104729.
- Smith D and Lipkin H (1990) Analysis of fourth order manipulator kinematics using conic sections. In: *Proceedings., IEEE International Conference on Robotics and Automation*. Cincinnati, OH, USA: IEEE Comput. Soc. Press. ISBN 978-0-8186-9061-7, pp. 274–278. DOI:10.1109/ROBOT.1990.125986.
- Thomas F (2015) A Distance Geometry Approach to the Singularity Analysis of 3R Robots. *Journal of Mechanisms and Robotics* 8(1): 011001. DOI:10.1115/1.4029500.
- Trinh C, Zlatanov D, Zoppi M and Molino R (2015) A Geometrical Approach to the Inverse Kinematics of 6R Serial Robots With Offset Wrists. In: *International Design Engineering Technical Conferences and Computers and Information in Engineering Conference*, volume Volume 5C: 39th Mechanisms and Robotics Conference. p. V05CT08A016.
- Verheyen A (2021) Why hasn't anyone heard of cuspidal robots? URL <https://tinyurl.com/achille-cuspidal>.
- Wächter A and Biegler LT (2006) On the implementation of an interior-point filter line-search algorithm for large-scale nonlinear programming. *Mathematical programming*.

